First-principles study of magnetism in spinel MnO_2

Dane Morgan and Billie Wang
Department of Materials Science and Engineering, Massachusetts Institute of Technology, Cambridge, Massachusetts 02139

Gerbrand Ceder
Department of Materials Science and Engineering and Center for Materials Science and Engineering, Massachusetts Institute of Technology, Cambridge, Massachusetts 02139

Axel van de Walle
Department of Materials Science and Engineering, Northwestern University, Evanston, Illinois 60208
(Received 3 September 2002; published 3 April 2003)

First-principles electronic structure methods have been used to calculate the ground state, transition temperature, and thermodynamic properties of magnetic excitations in spinel MnO_2. The magnetic interactions are mapped onto a Heisenberg model whose exchange interactions are fitted to results of first-principles calculations of different spin configurations. The thermodynamics are calculated using Monte Carlo methods. The Heisenberg model gives an extremely accurate representation of the true first-principles magnetic energies. We find a critical temperature and Weiss constant significantly larger than experimental results and believe the error to come from the local spin density approximation. We predict a new magnetic ground state different from that proposed previously, but consistent with experimental data.

DOI: 10.1103/PhysRevB.67.134404 PACS number(s): 75.10.Hk, 75.40.Mg

I. INTRODUCTION

Spinel MnO_2 (often referred to as λ-MnO_2) has very interesting and complex magnetic behavior. The nearest-neighbor interaction between Mn^{4+} ions has both ferromagnetic and antiferromagnetic contributions, which depend differently on the Mn^{4+}-Mn^{4+} distances.[1–3] Pure MnO_2 has been shown experimentally to be at least weakly antiferromagnetic.[1,3,4] However, other Mn^{4+} oxides, such as $Li_4Mn_5O_{12}$, have been found to be ferromagnetic due to slightly different distances between the Mn^{4+}-Mn^{4+} neighbors.[3] In this work we focus on the magnetic ordering in the pure MnO_2. The spinel structure of MnO_2 can be obtained by chemical[1,3] or electrochemical[4] delithiation of $LiMn_2O_4$. The structure, shown in Fig. 1, is cubic (space group Fd-$3m$, number 227) and the Mn reside on the 16d Wyckoff positions. The Mn arrangement is strongly frustrated in that the magnetic moments on the Mn ions can never have only antiparallel nearest-neighbor moments. In addition, it has been shown that in a model with only nearest-neighbor antiferromagnetic interaction between moments, the magnetic ground state of the MnO_2 spinel is infinitely degenerate.[5] Although in some cases entropic factors break degeneracy at nonzero temperatures, there is strong evidence that the classical nearest-neighbor Heisenberg model on the spinel lattice remains paramagnetic at all temperatures and there is no ordering.[5] Consequently, the magnetic ground state and thermodynamics of this system are not at all obvious, and an understanding of longer-range interactions is required to predict the ground-state magnetic configuration.

Greedan *et al.* refined magnetic neutron diffraction data on λ-MnO_2 to obtain an ordered antiferromagnetic ground state.[3] However, Jang *et al.* also found spin-glass behavior in λ-Li_xMnO_2 for $x=0.07$, 0.98, and 1.82.[4] Jang *et al.* suggest that λ-MnO_2 may consist of either separated antiferromagnetically ordered regions and spin-glass regions or a clustered spin glass, where the randomly oriented elements of the spin glass are not individual spins but ordered antiferromagnetic domains. Jang *et al.* believe that this complex magnetic behavior is due to the frustrated nature of the lattice and the presence of different sized moments associated with different Mn valence states, induced by residual Li.

For λ-MnO_2 the transition temperatures, Weiss constants, and effective moments measured by experiments up until his point are given in Table I. The consistently negative values of the Weiss constant demonstrate the antiferromagnetic nature of the interactions in this system.

In this paper we perform a first-principles study of the magnetic ground state and thermodynamics of λ-MnO_2. Section II contains a description of the theoretical approach used here and a comparison with other methods. Section III contains our results concerning the magnetic ground state

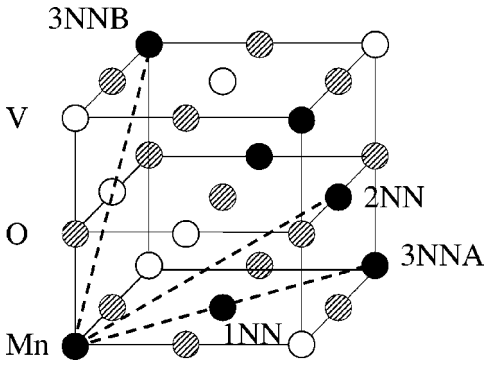

FIG. 1. The structure of spinel MnO_2 viewed as two interpenetrating fcc lattices. The first three nearest-neighbor pairs are labeled. The manganese (Mn), oxygen (O), and vacancies (V) are shown by filled, striped, and open circles, respectively.

TABLE I. Comparison between this work and previous experimental measurements of the MnO_2 magnetic transition temperature and Weiss constant.

Authors	Transition temperature (K)	Weiss constant (K)
Goodenough *et al.*[a]	40	−105
Greedan *et al.*[b]	32	−104
Jang *et al.*[c]	16	−74
This work	62	−210

[a]Reference 1.
[b]Reference 3.
[c]Reference 4.

and thermodynamics of λ-MnO_2, and Sec. IV gives a summary and conclusions.

II. THEORETICAL BACKGROUND

A. Heisenberg model

The most common approach to studying magnetism in solids with first-principles methods is to use density functional theory in the local spin density approximation (LSDA). Unfortunately, most calculations are limited to only collinear spins, which by itself is clearly inadequate for studying the spin thermodynamics, where many noncollinear spin configurations are relevant. There are well-developed techniques for the study of noncollinear magnetism with first-principles methods (for a fairly recent review see Ref. 6); however, directly calculating all the spin configurations needed for thermodynamic simulation (using, for example, Monte Carlo methods) would be extremely computationally intensive. Recently, techniques for first-principles spin dynamics have been developed,[7–10] but they have not yet obtained widespread usage in standard electronic structure codes and their effectiveness is still under investigation. A straightforward and more established approach to studying magnetic thermodynamics is to parametrize the first-principles magnetic energies with a Heisenberg model Hamiltonian simple enough to allow very rapid calculation of the energies of different spin configurations.[11–16] We have therefore chosen to represent the magnetic energies using a classical Heisenberg model[17] of the form

$$H = J_0 + J_i \mathbf{S}_i + \sum_{\langle i,j \rangle} J_{ij} \mathbf{S}_i \cdot \mathbf{S}_j , \tag{1}$$

where the summation is over all distinct pairs, $\mathbf{S}_i$ is the three-dimensional spin vector on site i, and J_{ij} is the exchange-coupling between the moments on sites i and j. J_0 is a constant term and J_i is an effective local field at site i. It can be shown that for clusters of spins that are transformed into each other by symmetry operations of the crystal (symmetry equivalent clusters) the associated coupling parameters must be equal.[18] Therefore, Eq. (1) can be rewritten as

$$H = J_0 + m_{\text{point}} J_{\text{point}} \overline{\mathbf{S}_i} + m_{1\text{NN}} J_{1\text{NN}} (\overline{\mathbf{S}_i \cdot \mathbf{S}_j})_{1\text{NN}} + m_{2\text{NN}} J_{2\text{NN}} (\overline{\mathbf{S}_i \cdot \mathbf{S}_j})_{2\text{NN}} + \cdots , \tag{2}$$

where the summation has been written out explicitly for all the symmetry inequivalent types of point and pair spin clusters in the Mn sublattice for spinel MnO_2. The overbar denotes the average value over all symmetry-equivalent clusters in the crystal. If we express energies per MnO_2 formula unit, then the m_x's denote the number of spin clusters of type x per a Mn atom.

B. Fitting the exchange-coupling parameters

There is a very extensive literature on different methods used to obtain the values of the exchange-coupling interactions (see Ref. 6 and references therein). In the present work we perform a least-squares fit of the unknown exchange interactions to a set of first-principles energies calculated for different collinear spin arrangements. This fitting approach has been used previously with good success to study a number of different systems.[11–13,15,16]

There are a number of weaknesses of this approach that should be mentioned. First, the Heisenberg model is only appropriate for localized electrons, and great care must be taken when applying it to itinerant magnets. However, MnO_2 is expected to have very well localized moments on the Mn atoms so the Heisenberg model is appropriate for this system.

Another problem is that the Heisenberg model is most accurate as a quantum-mechanical Hamiltonian, where the $\mathbf{S}_i$ are quantum-mechanical spin operators. However, there are difficulties using the fitting outlined above in the quantum-mechanical case because there is a complex correspondence between the Heisenberg Hamiltonian eigenstates and the first-principles collinear spin energies.[19] In addition, an accurate thermodynamic calculation with a three-dimensional quantum Heisenberg Hamiltonian is a very formidable problem. Therefore, although it is an uncontrolled approximation, we are forced to model the system with a classical Heisenberg model. It should be noted that in the limit of large spin values the quantum-mechanical Heisenberg model will behave classically. It is of some consolation that in MnO_2 the Mn have a fairly large magnetic moment and that we are therefore closer to the domain of applicability of the classical Heisenberg model than we would be for a simple spin-$\frac{1}{2}$ system.

Finally, a further approximation is made by fixing the spin magnitude on every Mn. This approximation could be lifted by expanding our Heisenberg model to allow for different-size spin vectors, but for MnO_2 the moments are unlikely to change dramatically between different Mn atoms and the errors associated with fixing the moments are not likely to be significant. As will be seen in Sec. III, the model and fitting used here yield a nearly perfect representation of the first-principles magnetic energies.

C. The first-principles method

All first-principles calculations were performed in the spin-polarized local density approximation (LDA) or gener-

alized gradient approximation (GGA) to the density-functional theory (DFT), as implemented in the Vienna *ab initio* simulation package (VASP).[20,21] This implementation uses ultrasoft pseudopotentials and a plane-wave basis for the representation of the wave functions. Calculations were converged to within a few milli-electron-volts per MnO_2 formula unit with respect to *k*-point sampling in the Brillouin zone and the number of plane-wave basis functions (for the primitive unit cell of 12 atoms we used a $5\times5\times5$ Monkhorst-Pack mesh centered at Γ and an energy cutoff of 405 eV).

We found that the magnetic results were very sensitive to volume and that the GGA seemed to predict a ferromagnetic ground state, which is clearly contrary to experiment. The experimental volume[22] of the primitive cell is 129.9 Å^3 and the calculated volumes of the ferromagnetic structure are 125.3 Å^3 (-3.5%) for the LDA and 137.5 Å^3 ($+5.9\%$) for the GGA. Therefore, it can be seen that although the LDA gave the usual underprediction of the volume, the GGA corrected too much and ended up with a volume even farther from experiment. In addition, there is evidence that using the LDA constrained to experimental volumes can correct errors associated with using the fully relaxed LDA or GGA directly.[23] Therefore, we have used the LDA and fixed the lattice parameter for all calculations to be equal to that given by experiment (8.04 Å).[24]

It was found that variations in the magnetic configuration led to only minimal changes in Mn positions. Hence we chose to freeze all the atomic positions to those found by fully relaxing the cell internal atom positions in a ferromagnetic cell. The changes in energy associated with this constraint were calculated explicitly for two distinct antiferromagnetic configurations and found to be less than 1 meV per formula unit for both cases.

D. The Monte Carlo method

The finite-temperature thermodynamic behavior has been calculated using standard Monte Carlo techniques. Simulations were performed with a $4\times4\times4$ or $6\times6\times6$ supercell of the conventional spinel cell (16 Mn ions per cell) containing a total of 1024 or 3456 spins, respectively. The number of Monte Carlo steps per spin was in the range 2000–5000 for each temperature, and of these the first 500–1000 were excluded from calculations of thermodynamic quantities to allow for equilibration. The size of the change in spin orientation attempted in a Monte Carlo step was adjusted as a function of temperature to keep the acceptance ratio approximately constant at about 50%. Similar simulation conditions have been used previously to study the Heisenberg model on this lattice.[5]

The specific heat was used to help identify the transition temperature and was calculated from the expression

$$C_v=(\langle E^2\rangle-\langle E\rangle^2)/NT^2, \tag{3}$$

where E is the total energy, N is the number of atoms, T is the temperature, and $\langle\cdots\rangle$ denotes the thermodynamic average of a quantity. The magnetic susceptibility was used to determine the Weiss constant and was calculated as

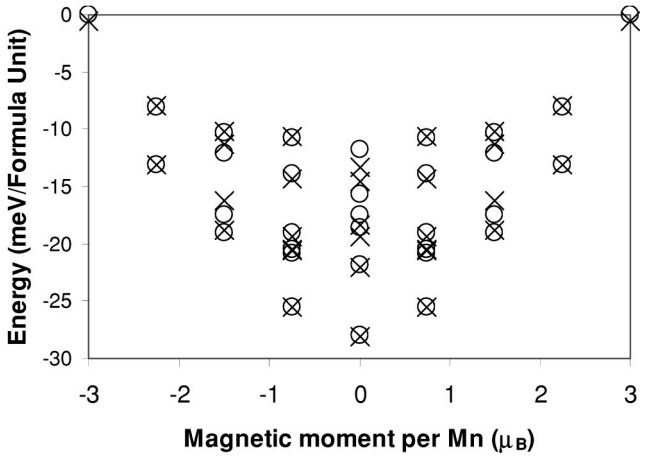

FIG. 2. The magnetic energies calculated by first principles (open circles) and predicted by the fitted Heisenberg model (crosses).

$$X=(\langle S^2\rangle-\langle S\rangle^2)/3NT, \tag{4}$$

where S is the magnitude of the sum of all spins on the lattice. The Weiss constant was found from the intercept with the abscissa of a linear fit to the high-temperature inverse susceptibility. At the relevant high temperatures, well above the magnetic phase transition, the value of $\langle S\rangle$ was taken to be zero. Note that although a renormalization of the spin magnitude, and therefore the susceptibility, would be necessary to allow direct comparison of susceptibility with experiment, the Weiss constant is independent of any rescaling of the susceptibility.

III. RESULTS

We calculated the energies of 19 different collinear magnetic configurations using cells of size 12 (primitive cell) or 24 (double cell) atoms. Note that in the following all energies are defined with respect to the ferromagnetic energy, which is taken to be zero. The unknown exchange couplings in the Heisenberg model [see Eq. (2)] were fitted to the 19 first-principles energies by minimizing the squared error between the calculated energies and those predicted by Eq. (2). It should be noted that all ''mirror'' pairs of spin orientations that can be obtained from each other by simply flipping over all the spins must have the same energy. This fact forces any coefficient in the Heisenberg Hamiltonian corresponding to an odd cluster of spins to be zero. In this case, the result is that the effective field (J_i) is zero, as would be expected. The first-principles and Heisenberg model predicted energies are shown together in Fig. 2. To bring out the correspondence with an energy versus composition plot commonly used in binary alloys, all ''mirror'' pairs are shown, which gives a total of 32 different points. Even with the limited number of interactions given in Fig. 1 the agreement is extremely good. The rms error between the first-principles and Heisenberg model predicted energies is less than 1 meV per formula unit.

The exchange-coupling parameters, along with the specific coordinates and separations of the atoms involved in each cluster, are given in Table II. Within the third-neighbor

TABLE II. The exchange terms and their associated pairs used in the Heisenberg model.

Exchange-coupling parameter	Value (meV)	Multiplicity (m_x)	Cluster coordinates (in fractional coordinates of conventional cell)	Pair separation (in units of lattice parameter)
J_0	−25.7	1		
J_{point}	0.0	1	$(\frac{5}{8},\frac{5}{8},\frac{5}{8})$	
$J_{1\text{NN}}$	4.9	3	$(\frac{5}{8},\frac{5}{8},\frac{5}{8})$ $(\frac{3}{8},\frac{3}{8},\frac{5}{8})$	0.3536
$J_{2\text{NN}}$	−0.9	6	$(\frac{5}{8},\frac{5}{8},\frac{5}{8})$ $(\frac{3}{8},\frac{9}{8},\frac{7}{8})$	0.6124
$J_{3\text{NN}A}$	5.1	3	$(\frac{5}{8},\frac{5}{8},\frac{5}{8})$ $(\frac{5}{8},\frac{9}{8},\frac{9}{8})$	0.7071
$J_{3\text{NN}B}$	0.1	3	$(\frac{5}{8},\frac{5}{8},\frac{5}{8})$ $(\frac{9}{8},\frac{9}{8},\frac{5}{8})$	0.7071

shell there are two inequivalent pairs, each at the same distance, and these have been labeled *A* and *B*. As there is no applied field the point term is forced to be zero by the equivalent energies of mirror pairs of configurations.

As might be expected, the first-neighbor coupling is antiferromagnetic. What is very surprising is that the *A*-type third-neighbor coupling is also antiferromagnetic and in fact the strongest interaction, whereas the *B*-type third-neighbor coupling is very weak. An obvious difference between the two types of third neighbors is that the *A* type has a shared nearest-neighbor Mn between them, whereas the *B*-type neighbors do not. It is possible that this intermediate Mn couples the two Mn in the *A*-type third neighbor in a strong antiferromagnetic manner.

The coupling parameters in Table II have been used in Monte Carlo simulations to calculate the thermodynamic properties for a range of temperatures. From the peak in the specific heat we identify a transition temperature of 62 K and a fit to the high-temperature inverse susceptibility gives a Weiss constant of −210 K. The transition temperature and Weiss constant are given in Table I along with experimental values. The calculated values are significantly high for both the ordering temperature and the Weiss constant, suggesting that our interactions are larger than those in the true system. Significant errors in the thermodynamic quantities may have been introduced by the approximations associated with using a classical Heisenberg model rather than a true quantum-mechanical spin Hamiltonian (see Sec. II B for more discussion of this approximation). The accuracy of the fitted model in reproducing the first-principles results suggests that the major source of the error lies in the first-principles energies. Some error may have been introduced by the volume issues discussed in Sec. II C. However, the error is not unexpected, since the LSDA has previously been shown to overestimate exchange interactions in similar systems, due to an overestimation of *p-d* hybridization.[13]

Table III shows the correlations as zero temperature is approached in the simulations. The correlations are the average spin variables used in Eq. (2). Also included in Table III are the correlations of the antiferromagnetic ground state proposed by Greedan *et al.*[3] The final column of Table III gives the energy predicted by our fitted Heisenberg Hamiltonian for each of the two ground states. It is clear that for our model Hamiltonian the structure suggested by Greedan *et al.* cannot be the ground state, as it has a very high energy.

The ground state found by Greedan *et al.* was obtained by refinement of magnetic neutron diffraction data. However, the refinement was initialized from only three candidate magnetic orderings, all based on the materials GeN_2O_4 and $GeCo_2O_4$, and the one that most closely matched the diffraction data was taken to be the ground state. The candidate ground state we identified was not considered as a possibility in the refinement by Greedan *et al.* As noted by Greedan *et al.*, the presence of only odd reflections requires a face-centered magnetic ordering where spins related by $(\frac{1}{2},\frac{1}{2},\frac{1}{2})$ translation must have opposite orientations. Our proposed ground state meets these conditions. Using the same magnetic neutron diffraction data as Greedan *et al.*, we have performed a refinement of our predicted magnetic structure using the FULLPROF software.[25] The following were simultaneously refined for both a magnetic MnO_2 phase and graphite impurity: a six-coefficient polynomial background,

TABLE III. Correlations and energy predicted from the fit Heisenberg model for two candidate ground states.

	Point	1NN	2NN	3NN *A*	3NN *B*	Energy (meV)
This work	0	0	0	−1	1	−40.8
Greedan *et al.*[a]	0	$\frac{1}{3}$	0	$\frac{1}{3}$	$-\frac{1}{3}$	−15.7

[a]Reference 3.

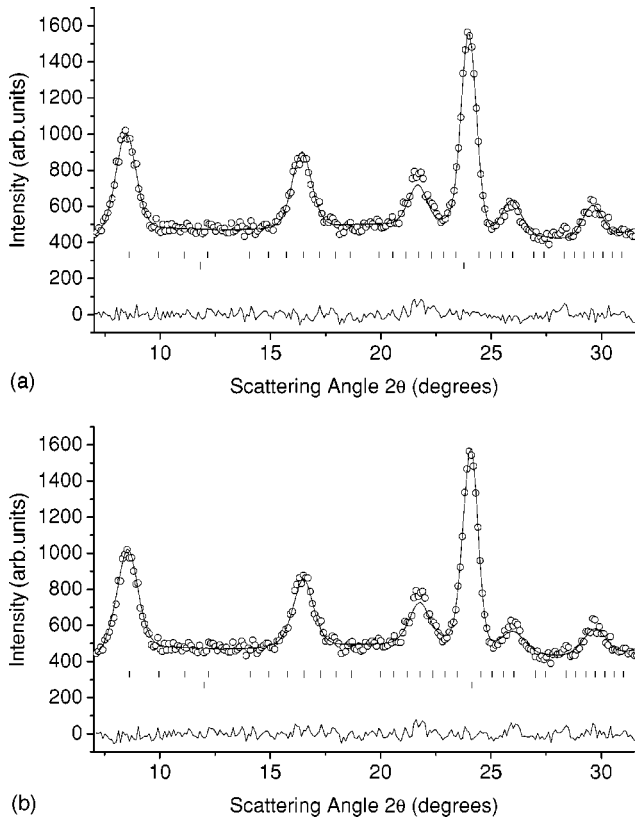

FIG. 3. The experimental (circles) and refined data (line) for proposed λ-MnO_2 magnetic structures: (a) this work; (b) Greedan *et al.* (Ref. 3).

pseudo-Voigt-peak shapes with asymmetry corrections, isotropic temperature factors, cell volumes, and scale factors. A total of 25 parameters (21 of which were independent) were refined, with 9 (7 of which were independent) associated with the graphite impurity and 16 (14 of which were independent) associated with the MnO_2 magnetic structure. The Mn atom positions were not refined since they are fixed by symmetry. No effort was made to refine the orientation of the magnetic moments since the proposed magnetic state has cubic symmetry (space group F-43m as calculated with the PLATON code[26]) and the powder pattern is therefore independent of moment orientation.[27]

The resulting refinement, shown in Fig. 3(a), gives a reasonably good agreement with the limited and somewhat noisy data ($\chi^2=1.22, R_{wp}=15.0\%$). Please see the FULLPROF[25] documentation for the exact definition of these error measurements. It is difficult to compare directly to the previous refinement of Greedan *et al.*, since they used a different program and may have included somewhat different effects in their refinement. However, a simple visual inspection suggests that we obtain comparable accuracy. To make a more quantitative comparison, we performed a refinement similar to that described above, but starting with the magnetic ground-state ordering suggested by Greedan, *et al.* All the parameters used in the refinement of our proposed ground state were included, as well as two additional parameters describing the relative angles of the magnetic moment axis with respect to the lattice vectors. The refinement starting with the Greedan *et al.* proposed magnetic ordering yielded $\chi^2=1.24$ and $R_{wp}=14.7\%$ and is shown in Fig. 3(b). The accuracy is essentially identical to that obtained refining our proposed structure. Based on the agreement with experimental diffraction data and the outcome from the first-principles calculations, we propose that the ground state produced by our simulations is consistent with the true antiferromagnetic tendencies of the λ-MnO_2 system. Note that we have made no attempt to explore the possibility of spin-glass formation at this time.

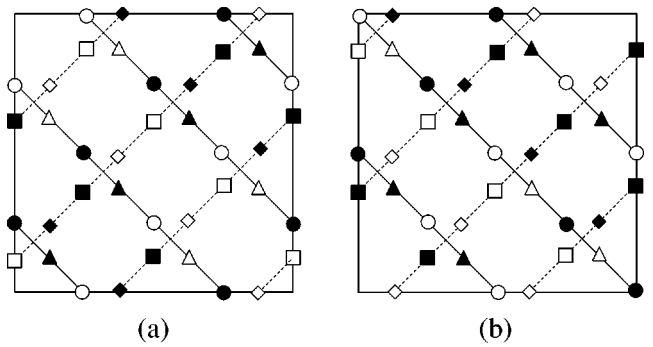

FIG. 4. The magnetic ground state obtained from our fitted Heisenberg model, drawn in a doubled conventional spinel unit cell. Only the Mn atom sites are shown. The circles, triangles, diamonds, and squares each represent a different "sublattice" of Mn atoms connected by third-nearest-neighbor pairs of type *A* (see Fig. 1). The filled and empty symbols represent up or down spins, respectively. The solid (dashed) lines give the $z=0$ ($x=\frac{1}{8}$) and $z=\frac{1}{4}$ ($z=\frac{3}{8}$) planes in (a) and (b), respectively (where coordinates are fractions of the double cell parameters). The spin orientations for $z \geqslant 0.5$ are not shown since a translation of (0,0,0.5) always reverses the spin.

The ground state proposed in this work is pictured in Fig. 4. In this figure all of the spins have been drawn collinearly. However, there are an infinite class of degenerate ground states with the same energy as that shown in the figure. The ground state can be pictured in the following way. Consider the four Mn atoms in the spinel primitive unit cell. Starting at each one of these Mn, move to other Mn by third-nearest-neighbor steps. Each of the four original Mn thereby defines an independent sublattice connected by third-nearest neighbors. Each sublattice has perfect antiferromagnetic order, in the sense that every *A*-type third neighbor is antiparallel to all its surrounding *A*-type third neighbors. This means that there is collinear order on each sublattice.

It is interesting to note that all relative orientation of the different sublattices with respect to one another are degenerate in energy. This can be seen quite easily for the nearest-neighbor couplings. For a given Mn atom the six nearest neighbors can be divided up into three pairs of *A*-type third-nearest neighbors. Since each of these pairs are exactly antiparallel with respect to each other, the surrounding nearest neighbors provide canceling interactions, regardless of the orientations of the sublattices. Another way to say this is that the nearest-neighbor correlation is zero independent of the orientation of the sublattices. A similar argument holds for the second-nearest neighbors. Therefore, although each sublattice is collinear within itself, the sublattices can orient ran-

domly relative to each other at no cost to the energy. In the real system, longer-range interactions and overall anisotropy might cause the sublattices to align.

IV. SUMMARY AND CONCLUSIONS

We have studied the magnetic behavior of spinel λ-MnO_2 using a Heisenberg model. The exchange-coupling parameters in the Heisenberg model were determined by a least-squares fit of energies predicted by the model to calculated first-principles energies. The Heisenberg model is able to reproduce the first-principles magnetic energies with a few milli-electron-volt accuracy using only the first few nearest-neighbor pair interactions. Monte Carlo methods were used to calculate the ordered ground state, transition temperature, and Weiss constant. The transition temperature and Weiss constant are significantly higher than experiment, most likely due to the known overestimation of exchange effects in LSDA calculations. On the basis of these first-principles results we propose a new ground state that is consistent with the experimental magnetic neutron diffraction data but different from the ground state proposed previously.[3] Previous refinements may have simply overlooked this ground state as a candidate structure.

ACKNOWLEDGMENTS

We would like to thank the Center for Materials Science and Engineering at MIT for their generous funding of this work. The authors acknowledge the support of the National Science Foundation (MRSEC Program) under Contract No. DMR 98-08941. Computing resources from NPACI, the National Partnership for Advanced Computing Infrastructure (NSF), are also gratefully acknowledged. We would also like to acknowledge valuable conversations with D. P. Landau, U. Amador, E. Arroyo, D. Carlier, A. Zunger, Clare Gray, and J. Greedan. We are particularly grateful to J. Greedan for generously providing us with the magnetic neutron diffraction data.

[1] J. B. Goodenough, A. M. Anthiram, A. C. W. P. James, and P. Strobel, in *Solid State Ionics*, Mater. Res. Soc. Symp. Proc. No. 135, edited by G. Nazri, R. A. Higgins, and D. F. Shriver (MRS, Warrendale, PA, 1989), p. 391.

[2] C. Masquelier, M. Tabuchi, K. Ado, R. Kanno, Y. Kobayashi, Y. Maki, O. Nakamura, and J. B. Goodenough, J. Solid State Chem. **123**, 255 (1996).

[3] J. E. Greedan, N. P. Raju, A. S. Wills, C. Morin, and S. M. Shaw, Chem. Mater. **10**, 3058 (1998).

[4] Y.-I. Jang, B. Huang, F. C. Chou, D. R. Sadoway, and Y.-M. Chiang, J. Appl. Phys. **87**, 7382 (2000).

[5] J. N. Reimers, Phys. Rev. B **45**, 7287 (1992).

[6] L. M. Sandratskii, Adv. Phys. **47**, 91 (1998).

[7] V. P. Antropov, M. I. Katsnelson, M. van Schilfgaarde, and B. N. Harmon, Phys. Rev. Lett. **75**, 729 (1995).

[8] V. P. Antropov, M. I. Katsnelson, B. N. Harmon, M. van Schilfgaarde, and D. Kusnezov, Phys. Rev. B **54**, 1019 (1996).

[9] B. Ujfalussy, X.-D. Wang, D. M. C. Nicholson, W. A. Shelton, and G. M. Stocks, J. Appl. Phys. **85**, 4824 (1999).

[10] Q. Niu, X. Wang, L. Kleinman, W.-M. Liu, D. M. C. Nicholson, and G. M. Stocks, Phys. Rev. Lett. **83**, 207 (1995).

[11] R. Dovesi, J. M. Ricart, V. R. Saunders, and R. Orlando, J. Phys.: Condens. Matter **7**, 7997 (1995).

[12] S. S. Peng and H. J. F. Jansen, Phys. Rev. B **43**, 3518 (1991).

[13] S.-H. Wei and A. Zunger, Phys. Rev. B **48**, 6111 (1993).

[14] N. M. Rosengaard and B. Johansson, Phys. Rev. B **55**, 14 975 (1997).

[15] Y.-M. Zhou, D.-S. Wang, and Y. Kawazoe, Phys. Rev. B **59**, 8387 (1999).

[16] J.-T. Wang, L. Zhou, D.-S. Wang, and Y. Kawazoe, Phys. Rev. B **62**, 3354 (2000).

[17] N. W. Aschroft and N. D. Mermin, *Solid State Physics* (Harcourt Brace, New York, 1976).

[18] J. Sanchez, F. Ducastelle, and D. Gratias, Physica A **128**, 334 (1984).

[19] I. P. R. Moreira and F. Illas, Phys. Rev. B **55**, 4129 (1997); F. Illas and R. L. Martin, J. Chem. Phys. **108**, 2519 (1998).

[20] G. Kresse and J. Furthmuller, Phys. Rev. B **54**, 11 169 (1996).

[21] G. Kresse and J. Furthmuller, Comput. Mater. Sci. **6**, 15 (1996).

[22] K. Kanamura, H. Naito, T. Yao, and Z. Takehara, J. Mater. Chem. **6**, 33 (1996).

[23] A. van de Walle and G. Ceder, Phys. Rev. B **59**, 14 992 (1999).

[24] K. Kanamura, H. Naito, T. Yao, and Z. Takehara, J. Mater. Chem. **6**, 33 (1996).

[25] J. Rodriguez-Carvajal, Physica B **192**, 55 (1993).

[26] A. L. Spek, PLATON, A Multipurpose Crystallographic Tool (Utrecht University, Utrecht, The Netherlands, 2001).

[27] G. E. Bacon, *Neutron Diffraction* (Clarendon, Oxford, 1975).